



Submitted: November 7, 2023

Revised: November 19, 2023

Accepted: December 8, 2023

Green's function molecular dynamics method for contact mechanics with a viscoelastic layer

V.G. Petrenko¹, I.U. Solovyov¹, E.V. Antonov¹ [✉], L.M. Dorogin¹,  Y. Murugesan²¹ ITMO University, St. Petersburg, Russia² University of Padova, Padua, Italy

✉ evantonov@itmo.ru

ABSTRACT

Advanced technological and engineering solutions involve usage of complex tribological systems. There is a demand for precise and computationally efficient methods to describe such systems. The aim of this study is to develop a computationally efficient method to solve the problem of deformation of a two-layer system using the Green's function molecular dynamics (GFMD) technique. We consider a viscoelastic layer attached to an elastic halfspace and derive a constitutive equation in Fourier space from the corresponding elastic solution. This third-order equation is numerically integrated by the backward Euler method, and a quasi-static solution is found through the fast inertial relaxation engine (FIRE) optimization algorithm. The method is illustrated with a simple model of indentation by a rigid cylinder. Using this method, contact area and pressure were calculated as a function of time for various shear modulus values.

KEYWORDS

boundary element method • viscoelasticity • contact mechanics • computational method • contact area

Acknowledgements. *The work was supported by the Ministry of Science and Higher Education of the Russian Federation (Project 075-15-2021-1349).*

Citation: Petrenko VG, Solovyov IU, Antonov EV, Dorogin LM, Murugesan Y. Green's function molecular dynamics method for contact mechanics with a viscoelastic layer. *Materials Physics and Mechanics*. 2024;52(1): 60-68. http://dx.doi.org/10.18149/MPM.5212024_6

Introduction

Tribology is one of the oldest sciences, yet even after the hundreds of years of research it remains not completely understood. Tribology of viscoelastic materials is becoming more and more important as technology moves forward: there is a large class of new rubber-like materials which have a wide range of innovative implementations in engineering, microelectronics, microbiology. Therefore, when modelling such systems, it is necessary to include an accurate description of the response of the viscoelastic material. The contact of a rigid rough surface with a viscoelastic halfspace was investigated in the work of Bugnicourt et al. [1]. In their work, the contact problem was numerically solved through a combination of the backward Euler method and conjugate gradient optimization. A viscoelastic model utilizing Green's function molecular dynamics (GFMD) and a semi-analytical solution with improved accuracy instead of the backward Euler method was developed in [2] and applied to the quasi-static indentation and rolling of a rigid cylinder on a frictionless viscoelastic halfspace. GFMD [3] is a boundary element method based on the fast Fourier transform and molecular dynamics energy minimization that simulates the response of an elastic body to an external force. GFMD has been used in simulations of rough elastic contacts [4], bodies of finite height [5], atomistic systems [3], viscoelastic

halfspaces [6] and adhesive viscoelastic roughness contact [7]. Recently, GFMD was accelerated with the fast inertial relaxation engine (FIRE) algorithm, resulting in speedups of one order of magnitude [8].

Contact mechanics models are used in many applications [9–11]. Sometimes contact mechanical systems can be represented by semi-infinite bodies. That, however, is not always the case [12]. There are systems that require a consideration of the layer's thickness, such as power transmission belts [13], seismic energy dissipation systems [14], electroadhesive devices [15], multi-layer structure [16], biomedical applications [17], coatings etc. In these situations, one should take into consideration the surface layer on top of the main half-space [18]. With further modification that concept can be used in investigation of adhesion of viscoelastic polymers depending on various factors, such as temperature, environment [19], blending [20] or molecular cross-linking density [21].

In this work we study the indentation of a viscoelastic layer of finite thickness bonded to an elastic halfspace. The paper is organized as following. In section "Methods", a constitutive equation is derived, following which, the methodology to obtain a numerical solution is explained. In section "Result and Discussion", using the newly developed model, the results for the indentation of a cylindrical punch onto a viscoelastic material are shown and discussed.

Methods

Consider a viscoelastic layer with stress σ and strain ε . Let $s = \sigma - (1/3) \text{tr}(\sigma) I$ be the stress deviator, and let $e = \varepsilon - (1/3) \text{tr}(\varepsilon) I$ be the strain deviator. Assume that viscoelasticity of the layer is described by the following equation [22]:

$$s(t) = \int_{-\infty}^t G(t-t') \dot{e}(t') dt', \quad (1)$$

where t is the time and $G(t)$ is the time-dependent shear modulus. The complex shear modulus $G(\omega)$ is then defined by

$$G(\omega) = i\omega \int_0^{\infty} G(t) e^{-i\omega t} dt', \quad (2)$$

so that

$$s(\omega) = 2G(\omega)e(\omega), \quad (3)$$

where $s(\omega) = \int e^{-i\omega t} s(t) dt$, $e(\omega) = \int e^{-i\omega t} e(t) dt$, and ω is the angular frequency.

The complex shear modulus in the Zener model [22] is given by

$$G(\omega) = (G_0 + i\omega\tau G_{\infty}) \times (1 + i\omega\tau)^{-1}, \quad (4)$$

where τ is the relaxation time, $G_0 = \lim_{\omega \rightarrow 0} G(\omega)$ is the low-frequency shear modulus, and $G_{\infty} = \lim_{\omega \rightarrow \infty} G(\omega)$ is the high-frequency shear modulus. The time-dependent shear modulus takes the form:

$$G(t) = G_0 + (G_{\infty} - G_0) e^{-t/\tau}. \quad (5)$$

Substituting Eq. (4) in Eq. (3) and applying an inverse Fourier transform, we obtain:

$$s(t) + \tau \dot{s}(t) = 2G_0 e(t) + 2\tau G_{\infty} \dot{e}(t). \quad (6)$$

For an elastic halfspace with shear modulus G and Poisson ratio ν the relation between normal surface stress $\sigma(x)$ and normal surface displacement $u(x)$ is [23]:

$$u(x) = -\frac{1-\nu}{2\pi G} \int \frac{\sigma(x')}{|x-x'|} dx'. \quad (7)$$

After taking the Fourier transform, we can write:

$$u(q) = M(q)\sigma(q), \quad (8)$$

where $u(q) = \int u(x) e^{-ix \cdot q} dx$, $\sigma(q) = \int \sigma(x) e^{-ix \cdot q} dx$, q is the wavevector, $q = |q|$, and

$$M(q) = -\frac{1-\nu}{Gq}. \quad (9)$$

Consider an elastic layer of thickness d with shear modulus G and Poisson ratio ν attached to an elastic halfspace with shear modulus G_{bulk} and Poisson ratio ν_{bulk} . Equation (9) becomes (see [24]):

$$M(q) = -\frac{1-\nu}{Gq} S(q), \quad (10)$$

where

$$S(q) = \frac{1+4mqde^{-2qd}-mne^{-4qd}}{1-(m+n+4mq^2d^2)e^{-2qd}+mne^{-4qd}}, \quad (11)$$

where

$$m = (G/G_{\text{bulk}} - 1) \times (G/G_{\text{bulk}} + 3 - 4\nu)^{-1}, \quad (12a)$$

$$n = 1 - \frac{4(1-\nu)}{1+(G/G_{\text{bulk}})(3-4\nu_{\text{bulk}})}. \quad (12b)$$

In the limiting case where the halfspace is rigid ($G_{\text{bulk}} = \infty$), Eq. (11) reduces to:

$$S(q) = \frac{(3-4\nu_0) \sinh(2qd) - 2qd}{(3-4\nu_0) \cosh(2qd) + 2(qd)^2 - 4\nu_0(3-2\nu_0) + 5}, \quad (13)$$

while for a free layer ($G_{\text{bulk}} = 0$), Eq. (11) reduces to:

$$S(q) = \frac{\sinh(2qd) + 2qd}{\cosh(2qd) - 2(qd)^2 - 1}. \quad (14)$$

Assume the layered solid is incompressible. Then $\nu = \nu_{\text{bulk}} = 0.5$ and Eq. (12) simplify to:

$$m = n = (G - G_{\text{bulk}})/(G + G_{\text{bulk}}). \quad (15)$$

Due to the elastic-viscoelastic correspondence principle, a solution to our viscoelastic problem can be derived from the elastic solution by replacing G with the complex shear modulus $G(\omega)$. Substituting Eq. (4) in Eq. (15) gives:

$$n = \frac{(G_0 + i\omega\tau G_\infty)/(1 + i\omega\tau) - G_{\text{bulk}}}{(G_0 + i\omega\tau G_\infty)/(1 + i\omega\tau) + G_{\text{bulk}}} = \frac{(G_0/G_{\text{bulk}} - 1) + i\omega\tau(G_\infty/G_{\text{bulk}} - 1)}{(G_0/G_{\text{bulk}} + 1) + i\omega\tau(G_\infty/G_{\text{bulk}} + 1)} = \frac{a_0 + sa_1}{a_2 + sa_3}, \quad (16)$$

where

$$s = i\omega\tau, \quad (17a)$$

$$a_0 = G_0/G_{\text{bulk}} - 1, \quad (17b)$$

$$a_1 = G_\infty/G_{\text{bulk}} - 1, \quad (17c)$$

$$a_2 = G_0/G_{\text{bulk}} + 1, \quad (17d)$$

$$a_3 = G_\infty/G_{\text{bulk}} + 1. \quad (17e)$$

We define:

$$r = e^{-2qd}, \quad (18a)$$

$$b_0 = -2(1 + 2(qd)^2), \quad (18b)$$

$$b_1 = 4qd, \quad (18c)$$

and write Eq. (11) as:

$$S(q) = \frac{1+4nqde^{-2qd}-(ne^{-2qd})^2}{1-(2n+4n(qd)^2)e^{-2qd}+(ne^{-2qd})^2} = \frac{1+b_1nr-(nr)^2}{1+b_0nr+(nr)^2}. \quad (19)$$

Substituting Eq. (16) gives:

$$S(q, \omega) = \frac{1+b_1((a_0+sa_1)/(a_2+sa_3))r - ((a_0+sa_1)/(a_2+sa_3))r^2}{1+b_0((a_0+sa_1)/(a_2+sa_3))r + ((a_0+sa_1)/(a_2+sa_3))r^2} = \quad (20)$$

$$\frac{(a_2+sa_3)^2 + b_1(a_0+sa_1)(a_2+sa_3)r - ((a_0+sa_1)r)^2}{(a_2+sa_3)^2 + b_0(a_0+sa_1)(a_2+sa_3)r + ((a_0+sa_1)r)^2} = \frac{c_{1,1} + c_{2,1}s + c_{3,1}s^2}{c_{1,0} + c_{2,0}s + c_{3,0}s^2},$$

where

$$c_{0,k} = 0, \quad (21a)$$

$$c_{1,k} = a_2^2 + a_0 a_2 b_k r + (-1)^k a_0^2 r^2, \quad (21b)$$

$$c_{2,k} = 2a_2 a_3 + (a_1 a_2 + a_0 a_3) b_k r + (-1)^k 2a_0 a_1 r^2, \quad (21c)$$

$$c_{3,k} = a_3^2 + a_1 a_3 b_k r + (-1)^k a_1^2 r^2, \quad (21d)$$

$$c_{4,k} = 0. \quad (21e)$$

For $k = 0, 1$. Using Eqs. (4), (9), and (20) gives:

$$M(q, \omega) = -\frac{S(q, \omega)}{2G(\omega)q} = -\frac{1}{2q} \frac{1+s}{G_0 + sG_\infty} \frac{c_{1,1} + c_{2,1}s + c_{3,1}s^2}{c_{1,0} + c_{2,0}s + c_{3,0}s^2} = -\frac{1}{2q} \frac{c_{1,1} + (c_{1,1} + c_{2,1})s + (c_{2,1} + c_{3,1})s^2 + c_{3,1}s^3}{G_0 c_{1,0} + (G_0 c_{2,0} + G_\infty c_{1,0})s + (G_0 c_{3,0} + G_\infty c_{2,0})s^2 + G_\infty c_{3,0}s^3}. \quad (22)$$

Substituting this in Eq. (8), we have:

$$\sum_{k=0}^3 (c_{k+1,1} + c_{k,1}) s^k \sigma(q, \omega) = -2q \sum_{k=0}^3 (c_{k+1,0} G_0 + c_{k,0} G_\infty) s^k u(q, \omega). \quad (23)$$

An inverse Fourier transform is applied to obtain the constitutive equation:

$$\sum_{k=0}^3 (c_{k+1,1} + c_{k,1}) \tau^k \partial_t^k \sigma(q, t) = -2q \sum_{k=0}^3 (c_{k+1,0} G_0 + c_{k,0} G_\infty) \tau^k \partial_t^k u(q, t). \quad (24)$$

Consider the limiting case where the elastic halfspace is infinitely rigid, i.e., $G_{\text{bulk}} = \infty$. Then $-a_0 = -a_1 = a_2 = a_3 = 1$ and:

$$1 - b_k r + (-1)^k r^2 = c_{1,k} = c_{2,k}/2 = c_{3,k}. \quad (25)$$

For $k = 0, 1$ so that the left-hand side operator of Eq. (24) is:

$$\sum_{k=0}^3 (c_{k+1,1} + c_{k,1}) (\tau \partial_t)^k = c_{1,1} + (c_{1,1} + c_{2,1}) (\tau \partial_t) + (c_{2,1} + c_{3,1}) (\tau \partial_t)^2 + c_{3,1} (\tau \partial_t)^3 = (1 - b_1 r - r^2) (1 + 3(\tau \partial_t) + 3(\tau \partial_t)^2 + (\tau \partial_t)^3) = (1 - b_1 r - r^2) (1 + \tau \partial_t)^3, \quad (26)$$

while the right-hand side operator is:

$$-2q \sum_{k=0}^3 (c_{k+1,0} G_0 + c_{k,0} G_\infty) (\tau \partial_t)^k = -2q (1 - b_0 r + r^2) (G_0 + (2G_0 + G_\infty) (\tau \partial_t) + (G_0 + 2G_\infty) (\tau \partial_t)^2 + G_\infty (\tau \partial_t)^3) = -2q (1 - b_0 r + r^2) (G_0 + G_\infty \tau \partial_t) (1 + \tau \partial_t)^2. \quad (27)$$

After removing the common factor $(1 + \tau \partial_t)^2$, we get the equation:

$$\sigma(q, t) + \tau \dot{\sigma}(q, t) = -2q \frac{1 - b_0 r + r^2}{1 - b_1 r - r^2} (G_0 u(q, t) + G_\infty \tau \dot{u}(q, t)). \quad (28)$$

If the viscoelastic layer is infinitely thick, i.e., $d = \infty$, then Eq. (28) reduces to:

$$\sigma(q, t) + \tau \dot{\sigma}(q, t) = -2q (G_0 u(q, t) + G_\infty \tau \dot{u}(q, t)), \quad (29)$$

which was obtained and integrated semi-analytically by van Dokkum et al. [2]. Note that the same semi-analytical integration scheme may be used to solve Eq. (28).

Assume the layered solid is indented by rigid punch with a trajectory $h(x, t)$. The time is discretized into time points $0, \Delta t, 2\Delta t, \dots$ and the surface of the layered solid $u(x, t)$ is discretized with n grid points x_0, x_1, \dots, x_{n-1} . Overlap of the punch and the layered solid is not allowed ($u(x_j, t) \leq h(x_j, t)$). Also, it is assumed that at the bottom of the elastic solid being approximated by the elastic halfspace the displacements are fixed at zero. Then, since the layered solid is incompressible, the mean surface displacement is zero ($\sum_{j=0}^{n-1} u(x_j, t) = 0$).

To numerically solve Eq. (24) for σ the $\partial_t^k u$ are approximated with finite differences and used to compute the input to the backward Euler method. An alternative might be to solve Eq. (24) semi-analytically [25] for improved convergence properties. The equilibrium displacement field at a given time is found by solving an energy minimization problem via FIRE-based GFMD [8].

If $u(q, t - 4\Delta t)$, $u(q, t - 3\Delta t)$, $u(q, t - 2\Delta t)$, and $u(q, t - \Delta t)$ have been found, then $\sigma(q, t)$ can be shown to be a linear function of $u(q, t)$. Thus, the slopes and the intercepts of the linear functions may be precomputed before the minimization. (Note that the displacements could be shifted to eliminate the intercepts.)

The fast Fourier transform and its inverse are denoted by *FFT* and *IFFT*. The pseudocode is as follows:

```

0   set up the trajectory of the punch  $h(t)$ 
1   set displacements  $u(t)$  to zero for  $t < 0$ 
2    $t \leftarrow 0$ 
3    $be\_solver \leftarrow$  (backward Euler solver of (24) for  $\sigma$ )
4   while true
5    $a \leftarrow$  (slopes of  $\sigma$  from  $be\_solver$ )
6    $b \leftarrow$  (intercepts of  $\sigma$  from  $be\_solver$ )
7   use FIRE-based GFMD to find  $u(t)$  such that the energy corresponding to the force
    $IFFT(a \odot FFT(u(t)) + b)$  is minimal subject to  $\sum_{j=0}^{n-1} u(x_j, t) = 0$  and  $u(t) \leq h(t)$ , where
    $\odot$  is elementwise product
8    $rhs \leftarrow$  (new values of the right-hand side of (24) computed from  $u(t - 3\Delta t)$ ,
    $u(t - 2\Delta t)$ ,  $u(t - \Delta t)$ ,  $u(t)$  using finite differences)
9   update  $be\_solver$  with  $rhs$ 
10   $t \leftarrow t + \Delta t$ 

```

Results and Discussion

We consider indentation by a rigid punch in two dimensions. The punch is periodic in the x direction with period L and its trajectory is defined by:

$$h(x, t) = \frac{R}{2} \left(\frac{x}{R} \right)^2 + \frac{-h_0 L}{\tau} \cdot \begin{cases} 0, & \text{for } t < 0 \\ t, & \text{for } 0 \leq t < \tau, \\ \tau, & \text{for } t \geq \tau \end{cases} \quad (30)$$

for $-1/2 \leq x/L \leq 1/2$, where $h_0 L$ is the maximum indentation depth and R is the radius of curvature at $x = 0$. A schematic of the system is shown in Fig. 1. The relative contact area is defined as $\tilde{a} = a/L$, and the dimensionless pressure is defined as $\tilde{p} = \bar{p}(2G_0)$, where \bar{p} is the mean normal contact stress. The numerical results are obtained for $G_{\text{bulk}}/G_0 = 1$, $G_\infty/G_0 = 10$, $n = 2^{14} = 16384$, $h_0 = 0.01$, $R/L = 0.25$, $d/L = 0.05$, and $\Delta t/\tau = 0.005$ unless specified otherwise. Figure 2 shows \tilde{p} and \tilde{a} for $G_{\text{bulk}} = G_\infty$ and $d/L = 0, 1/32, 1/16, 1/8, 1/4, \infty$.

The relative contact area and the dimensionless pressure as functions of time for $G_\infty = G_{\text{bulk}}$ and $d/L = 0, 1/32, 1/16, 1/8, 1/4, \infty$ are presented in Figs. 2. At time $t \approx 0$ the responses are approximately the same. This is because the coating is responding with the high-frequency modulus $G_\infty = G_{\text{bulk}}$ and the whole layered solid is behaving like a purely elastic halfspace with $G = G_{\text{bulk}}$ regardless of thickness d . As the coating thickness d/L is varied from 0 to ∞ , the relative contact area curve rises until $d/L = 1/16$ and then returns to the initial values. As we can see, the contact area curve is the same for $d = 0$ and $d = \infty$. At $d = 0$ the system is purely elastic, hence the contact area and pressure become constant when the punch stops at $t = \tau$. The constantness of contact area at the hold for $d = \infty$ is in accordance with the simulations by van Dokkum [5]. That $\lim_{t \rightarrow \infty} \tilde{a}(t)$ must be the same for $d = 0$ and $d = \infty$ follows from the corresponding elastic energy functions being equal

up to a positive constant factor. In Figure 3, the contact area and the pressure for varying hardness of the bulk layer are presented. As the bulk becomes harder, the values of the contact area curve increase up to infinite rigidity, at which point the contact area is constant at the hold. In Figure 4, the contact area and the pressure for $G_\infty/G_0 = 2, 3, 5, 9, 17$ are presented. As G_∞ increases, the contact area curve goes down, while the pressure curve goes up. When $t \rightarrow \infty$, the curves approach the same response of an elastic halfspace with $G = G_0 = G_{\text{bulk}}$.

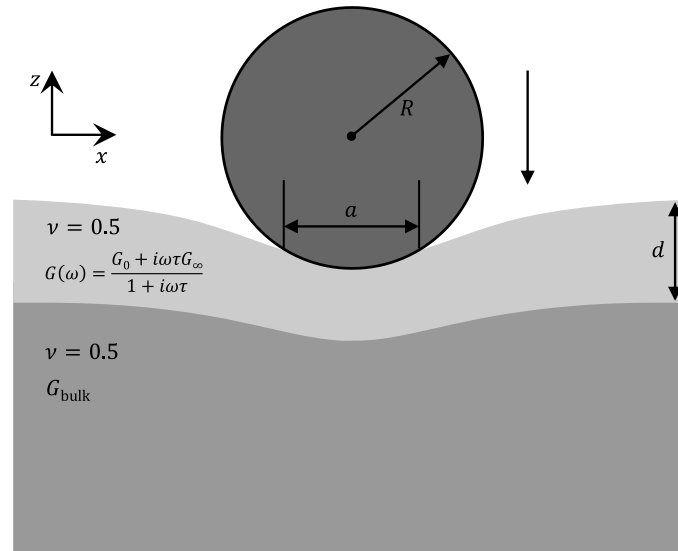


Fig. 1. Schematic of a rigid punch indenting a viscoelastically layered solid

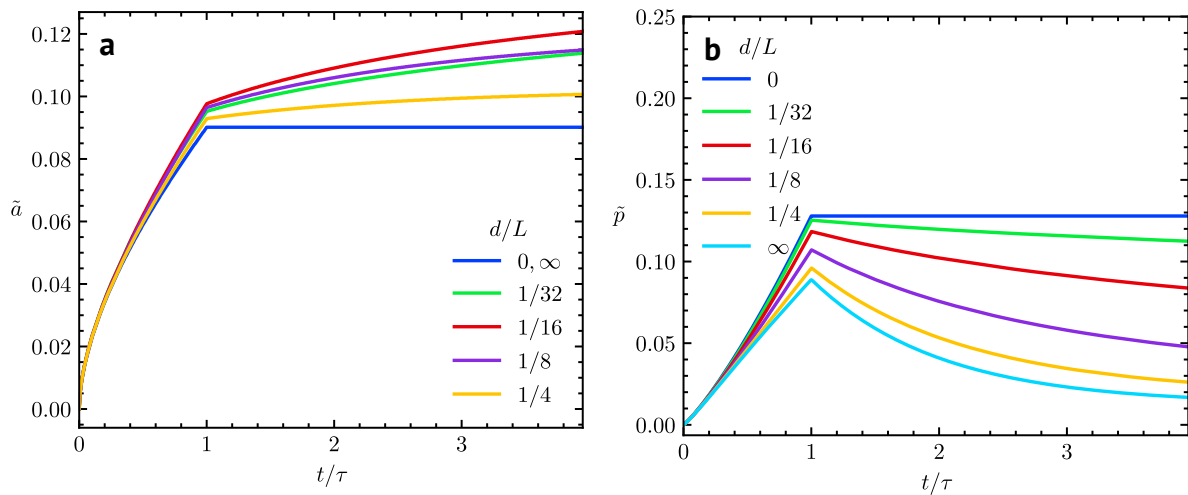


Fig. 2. The relative contact area \tilde{a} (a) and the dimensionless pressure \tilde{p} (b) as a function of the dimensionless time t/τ for $G_\infty = G_{\text{bulk}}$ and $d/L = 0, 1/32, 1/16, 1/8, 1/4, \infty$

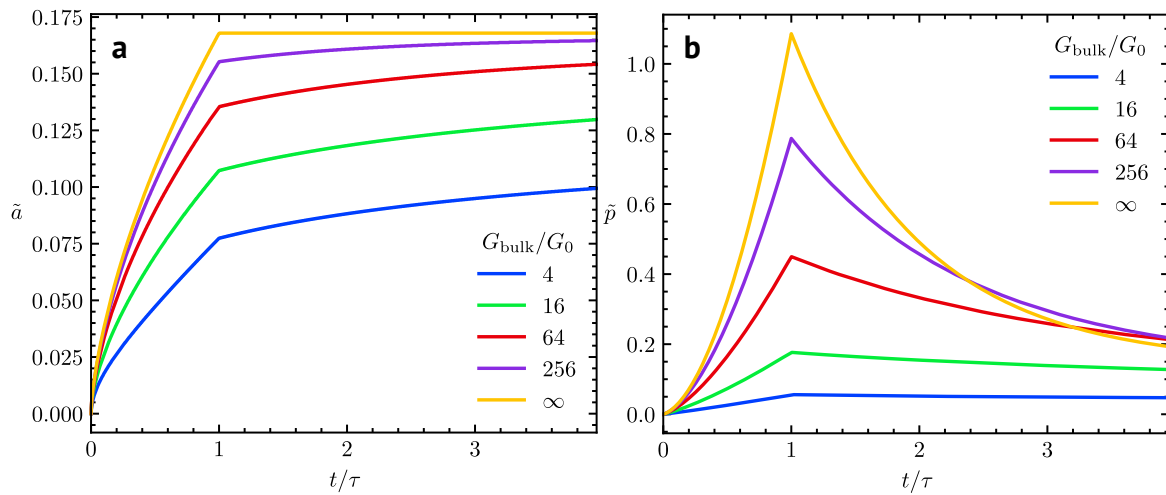


Fig. 3. The relative contact area \tilde{a} (a) and the dimensionless pressure \tilde{p} (b) as a function of the dimensionless time t/τ for $G_{\text{bulk}}/G_0 = 4, 16, 64, 256, \infty$

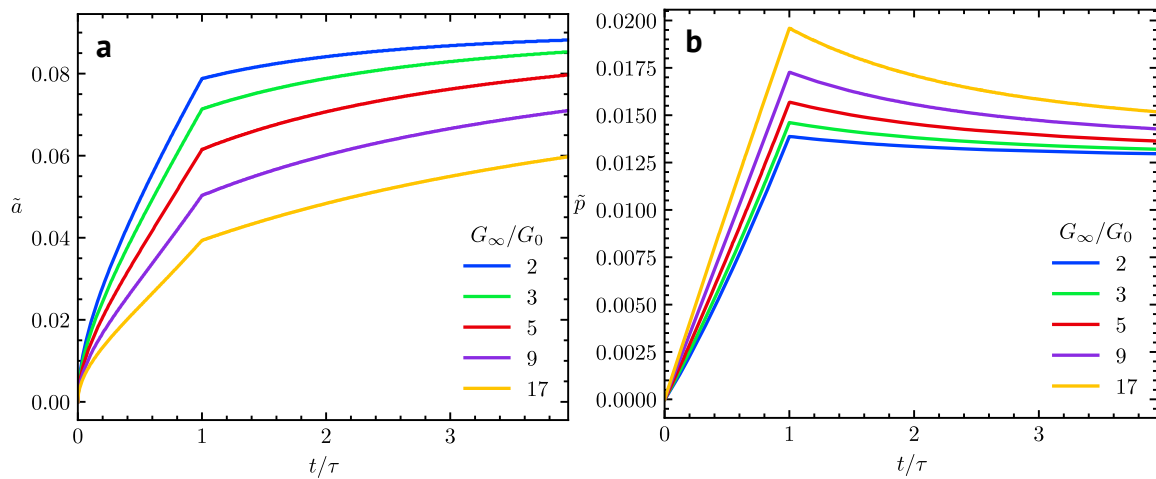


Fig. 4. The relative contact area \tilde{a} (a) and the dimensionless pressure \tilde{p} (b) as a function of the dimensionless time t/τ for $G_{\infty}/G_0 = 2, 3, 5, 9, 17$

Conclusions

There is a demand for computationally efficient methods to model tribological systems. We formulate and implement a GFMD technique to compute the response of a viscoelastic layer of finite thickness bonded to an elastic half-space. We derive a constitutive equation and solve it numerically using the backward Euler method. A quasi-static solution is found using the FIRE optimization algorithm. The developed method is applied to model indentation by a rigid punch.

The model described in the article can be used in a number of cases, for instance, electroadhesive devices, multi-layer structures, coating, and etc. Moreover, as a future development, this computational model can be extended with adhesion forces, more precise (higher orders) of viscoelastic material allowing to simulate broader range of cases.

References

1. Bugnicourt R, Sainsot P, Lesaffre N, Lubrecht AA. Transient frictionless contact of a rough rigid surface on a viscoelastic half-space. *Tribology International*. 2017;113: 279–285.
2. Dokkum JS van, Nicola L. Green's function molecular dynamics including viscoelasticity. *Modelling and Simulation in Materials Science and Engineering*. 2019;27(7): 075006.
3. Campañá C, Müser MH. Practical Green's function approach to the simulation of elastic semi-infinite solids. *Physical Review B*. 2006;74(7): 075420.
4. Prodanov N, Dapp WB, Müser MH. On the Contact Area and Mean Gap of Rough, Elastic Contacts: Dimensional Analysis, Numerical Corrections, and Reference Data. *Tribology Letters*. 2013;53(2): 433–448.
5. Venugopalan SP, Nicola L, Müser MH. Green's function molecular dynamics: including finite heights, shear, and body fields. *Modelling and Simulation in Materials Science and Engineering*. 2017;25(3): 034001.
6. Sukhomlinov S, Müser MH. On the viscous dissipation caused by randomly rough indenters in smooth sliding motion. *Applied Surface Science Advances*. 2021;6: 100182.
7. Pérez-Ràfols F, Van Dokkum JS, Nicola L. On the interplay between roughness and viscoelasticity in adhesive hysteresis. *Journal of the Mechanics and Physics of Solids*. 2023;170: 105079.
8. Zhou Y, Moseler M, Müser MH. Solution of boundary-element problems using the fast-inertial-relaxation-engine method. *Physical Review B*. 2019;99(14): 144103.
9. Sethi SK, Shankar U, Manik G. Fabrication and characterization of non-fluoro based transparent easy-clean coating formulations optimized from molecular dynamics simulation. *Progress in Organic Coatings*. 2019;136: 105306.
10. Müller C, Samri M, Hensel R, Arzt E, Müser MH. Revealing the coaction of viscous and multistability hysteresis in an adhesive, nominally flat punch: A combined numerical and experimental study. *Journal of the Mechanics and Physics of Solids*. 2023;174: 105260.
11. Müser MH, Dapp WB, Bugnicourt R, Sainsot P, Lesaffre N, Lubrecht TA, Persson BNJ, Harris K, Bennett A, Schulze K, Rohde S, Ifju P, Sawyer WG, Angelini T, Esfahani HA, Kadkhodaei M, Akbarzadeh S, Wu JJ, Vorlauffer G, Vernes A, Solhjoo S, Vakis AI, Jackson RL, Xu Y, Streator J, Rostami A, Dini D, Medina S, Carbone G, Bottiglione F, Afferrante L, Monti J, Pastewka L, Robbins MO, Greenwood JA. Meeting the Contact-Mechanics Challenge. *Tribology Letters*. 2017;65(4): 118.
12. Menga N, Afferrante L, Carbone G. Effect of thickness and boundary conditions on the behavior of viscoelastic layers in sliding contact with wavy profiles. *Journal of the Mechanics and Physics of Solids*. 2016;95: 517–529.
13. Zhu H, Zhu WD, Fan W. Dynamic modeling, simulation and experiment of power transmission belt drives: A systematic review. *Journal of Sound and Vibration*. 2021;491: 115759.
14. Zhang C, Ali A. The advancement of seismic isolation and energy dissipation mechanisms based on friction. *Soil Dynamics and Earthquake Engineering*. 2021;146: 106746.
15. Cao C, Sun X, Fang Y, Qin QH, Yu A, Feng XQ. Theoretical model and design of electroadhesive pad with interdigitated electrodes. *Materials & Design*. 2016;89: 485–491.
16. He T, Duan M, Wang J, Lv S, An C. On the external pressure capacity of deepwater sandwich pipes with inter-layer adhesion conditions. *Applied Ocean Research*. 2015;52: 115–124.
17. Guo S, Zhu X, Loh XI. Controlling cell adhesion using layer-by-layer approaches for biomedical applications. *Materials Science and Engineering: C*. 2017;70: 1163–1175.
18. Liu L, Yu M, Lin H, Foty R. Deformation and relaxation of an incompressible viscoelastic body with surface viscoelasticity. *Journal of the Mechanics and Physics of Solids*. 2017;98: 309–329.
19. Chipara AC, Tsafack T, Owuor PS, Yeon J, Junkermeier CE, Van Duin ACT, Bhowmick S, Asif SAS, Radhakrishnan S, Park JH, Brunetto G, Kaiparettu BA, Galvao DS, Chipara M, Lou J, Tsang HH, Dubey M, Vajtai R, Tiwary CS, Ajayan PM. Underwater adhesive using solid–liquid polymer mixes. *Materials Today Chemistry*. 2018;9: 149–157.
20. Sethi SK, Soni L, Shankar U, Chauhan RP, Manik G. A molecular dynamics simulation study to investigate poly(vinyl acetate)-poly(dimethyl siloxane) based easy-clean coating: An insight into the surface behavior and substrate interaction. *Journal of Molecular Structure*. 2020;1202: 127342.
21. Jin C, Wang Z, Volinsky AA, Sharfeddin A, Gallant ND. Mechanical characterization of crosslinking effect in polydimethylsiloxane using nanoindentation. *Polymer Testing*. 2016;56: 329–336.
22. Popov VL. *Contact mechanics and friction*. 2nd ed. Berlin, Germany: Springer; 2017.
23. Landau LD, Pitaevskii LP, Lifshitz EM, Kosevich AM. *Theory of elasticity*. 3rd ed. Oxford, England: Butterworth-Heinemann; 1984.

24. Persson BNJ. Contact mechanics for layered materials with randomly rough surfaces. *Journal of Physics: Condensed Matter*. 2012;24(9): 095008.
25. Sorvari J, Hämmäläinen J. Time integration in linear viscoelasticity—a comparative study. *Mechanics of Time-Dependent Materials*. 2010;14(3): 307–328.

About Authors

Veniamin G. Petrenko

PhD Student (ITMO University, St. Petersburg, Russia)

Ivan U. Solovyov

Engineer (ITMO University, St. Petersburg, Russia)

Evgenii V. Antonov

Engineer (ITMO University, St. Petersburg, Russia)

Leonid M. Dorogin

PhD, Associate Professor (ITMO University, St. Petersburg, Russia)

Yaswanth Murugesan

Engineer (University of Padova, Padua, Italy)